Physics of Liquefaction Phenomena around Marine Structures

M. B. de Groot[1]; M. D. Bolton[2]; P. Foray[3]; P. Meijers[4]; A. C. Palmer[5]; R. Sandven[6]; A. Sawicki[7]; and T. C. Teh[8]

Abstract: Understanding of the physical backgrounds is essential for good engineering practice with respect to liquefaction of sandy soils around and beneath marine structures. Several types of liquefaction can be distinguished. The corresponding physical phenomena are briefly described. Among them are: compressibility of soil skeleton, dilation, contraction, elastic versus plastic deformation, interaction between pore water and soil skeleton, compressibility of pore water, monotonic versus cyclic response, instantaneous versus residual liquefaction, drainage and pre-shearing. In each particular case just a limited number of these phenomena is relevant and needs to be modeled. A survey of typical cases is presented and the relevant phenomena are discussed. Most will be elaborated on in other papers appearing in this issue. This paper may help to discover the relationship between the different papers.

DOI: 10.1061/(ASCE)0733-950X(2006)132:4(227)

CE Database subject headings: Contracts; Cyclic loads; Drainage; Pore pressure; Liquefaction; Offshore structures.

Introduction

Aim of Paper

Liquefaction is the act or process of transforming any substance into a liquid. It often plays an important role around and beneath marine structures, as it may appear in saturated or nearly saturated granular materials, like seabed sand, under circumstances such as severe storms and earthquakes. The resulting loss of soil strength may have catastrophic consequences, such as large horizontal displacements of pipelines on the seabed, floating up of buried pipelines, tilting of caissons, and shear failure of breakwater slopes.

[1]GeoDelft, P.O. Box 69, 2600 AB Delft, The Netherlands (corresponding author). E-mail: m.b.degroot@geodelft.nl

[2]Dept. of Engineering, Univ. of Cambridge, Trumpington St., Cambridge CB2 1PZ, U.K. E-mail: mdb@eng.cam.ac.uk

[3]Laboratoire Sols, Solides, Structures, Domaine Univ., BP 53 38041 Grenoble Cedex, France. E-mail: pierre.foray@hmg.inpg.fr

[4]GeoDelft, P.O. Box 69, 2600 AB Delft, The Netherlands. E-mail: p.meijers@geodelft.nl

[5]Dept. of Engineering, Univ. of Cambridge, Trumpington St., Cambridge CB2 1PZ, U.K. E-mail: acp24@eng.cam.ac.uk

[6]Dept. of Geotechnical Engineering, NTNU, Institutt for Geoteknikk Høgskoleringen 7, 7491 Trondheim, Norway. E-mail: rolf.sandven@bygg.ntnu.no

[7]Institute of Hydroengineering, Polish Academy of Sciences, Koscierska 7, 80-953 Gdansk, Poland. E-mail: as@ibwpan.gda.pl

[8]Dept. of Engineering, Univ. of Cambridge, Trumpington St., Cambridge CB2 1PZ, U.K. E-mail: tcteh@cantab.net

Note. Discussion open until December 1, 2006. Separate discussions must be submitted for individual papers. To extend the closing date by one month, a written request must be filed with the ASCE Managing Editor. The manuscript for this paper was submitted for review and possible publication on May 11, 2004; approved on May 3, 2005. This paper is part of the ***Journal of Waterway, Port, Coastal, and Ocean Engineering***, Vol. 132, No. 4, July 1, 2006. ©ASCE, ISSN 0733-950X/2006/4-227–243/$25.00.

The professional geotechnical literature on liquefaction is already very rich, as extensive investigations in this area of research have been carried out for more than 30 years (see Sawicki and Mierczynski 2006). A famous older state-of-the-art paper is the 33rd Rankine Lecture by Ishihara (1993). More recent general information can be found in Youd et al. (2001). However, unlike for the example the theory of limit states or the theory of consolidation, the knowledge about liquefaction-related phenomena has not yet found a place in most geotechnical textbooks. This also means that the marine engineering community is not well acquainted with liquefaction related problems. A further limitation for marine engineering is the relatively limited attention paid in literature to wave induced liquefaction, which is characterized by specific phenomena not very relevant for earthquake induced liquefaction, like instantaneous liquefaction, drainage, and preshearing.

Marine engineers will need some basic knowledge about the physics of liquefaction in order to know when they should seek support from geotechnical specialists and to have fruitful cooperation with them. The aim of this paper is to provide some physical background regarding the liquefaction of (nearly) saturated, noncohesive soils, as well as related phenomena like pore-pressure accumulation, dissipation, and pore-pressure reduction during impact loading. Knowledge about the physical background is needed to assess the risk of such a liquefaction induced reduction of the foundation strength that large deformations or complete failure may occur. This paper should also help in understanding the papers published in this and the next issue of the journal.

Focus on Response of Soil Elements, Types of Liquefaction, Sandy Soils

The assessment of the liquefaction potential of the soil around a marine structure requires an extensive analysis of the loading conditions, such as those caused by waves and earthquakes. It also requires extensive knowledge of the interaction between structure and water, between structure and soil, as well as

between water and soil, due to these loads. The load distribution in the soil or the interaction between different parts of the soil, e.g., different layers, also needs to be analyzed in order to find the (loading) boundary conditions of specific soil elements and the response of these elements to these conditions.

These issues will not be discussed extensively in this paper. Most attention is paid to the (loading) boundary conditions of individual soil elements and the response of the elements to these conditions. Where, at the end of this paper, examples of the response of a soil–water–structure system, as a whole, to loading conditions are discussed, it is just for illustration of the phenomena elaborated on in the first parts of the paper.

Several types of liquefaction can be distinguished depending on the type of boundary conditions—monotonic or cyclic loading, normal or shear loading, easy drainage, or no drainage and depending on soil properties, like density and gas content. The combinations of specific physical phenomena defining these types will be discussed. As in other fields of physics, liquefaction can only be described if a limited number of such phenomena are assumed to be relevant.

This paper only deals with noncohesive soils, like sand, silt and gravel, usually described as "sandy soil" or even "sand." This limitation is partly for reasons of simplicity, and partly because sandy soils are generally the most sensitive to liquefaction. It should be realized that certain clays show similar behavior under certain circumstances. For a comprehensive study on the liquefaction of cohesive sediments reference is made to De Wit (1995).

Definition and Explanation of Liquefaction of Noncohesive Soils

In their "Summary Report from 1996 NCEER and 1998 NCEER/NSF Workshops on Evaluation of Liquefaction Resistance of Soils," Youd et al. (2001) refer, for the definition of liquefaction, to Marcuson (1978). The last committee defines liquefaction as "The act or process of transforming any substance into a liquid." The committee adds: "In cohesionless soils, the transformation is from a solid state to a liquefied state as a consequence of increased pore pressure and reduced effective stress." This addition corresponds to the following intuitive, very persuasive, explanation of liquefaction of (nearly) saturated noncohesive soils.

A noncohesive soil can be considered as an assembly of grains (soil skeleton) the pores of which are filled with water and or gas. The soil skeleton behaves macroscopically as a solid material, provided that there exist intergranular contacts enabling shear forces to be transferred. Because of this shear strength the skeleton can support additional loads as, for example, loads caused by marine structures.

The intergranular contacts in noncohesive soils can only transfer shear forces through friction if they transfer normal forces at the same time. Normal forces can be transferred through the skeleton, but also through the pore water. Thus, normal effective stress and pore pressure are the two components of the total normal stress. Liquefaction occurs when the total stress remains constant and the pore pressure increases such that the normal effective stress becomes zero. It also occurs when the pore pressure remains constant and the total stress decreases such that the normal effective stress becomes zero, as will be explained with the help of Figs. 29–31. The intergranular forces disappear and the shear stress that can be transferred becomes zero as well, when the normal effective stress becomes zero. Then, the soil cannot support any external load, except for a pure isotropic pressure, which is characteristic for liquids and other fluids.

Thus, liquefaction requires considerable "excess pore pressure." Excess pore pressure is defined here as the difference between the actual pore pressure and the hydrostatic pressure for still water level. Liquefaction with an excess pore pressure high enough to reduce the soil strength to zero, does not occur very often around marine structures. Excess pore pressure, however, frequently causes a significant decrease in shear resistance of part of the soil, which may result in a large deformation or even shear failure of the foundation. The term "liquefaction" will be used here for all such situations, even if the soil still has some shear resistance and does not behave like a Newtonian fluid. The terms "partial liquefaction" versus "full" or "complete liquefaction" will be used to distinguish between both conditions.

Soil Considered as Two-Phase Medium

In the case of saturated noncohesive soils, one deals with a two-phase medium. The two phases are soil skeleton and pore water. From a macroscopic point of view, such a mixture consists of two continua, superimposed on each other. This means that at each point of such an idealized mixture, there exist two phases, a solid (the skeleton) and a liquid (the pore water).

The pore water in most seabed sands is not completely saturated and contains small quantities of gas bubbles. Consequently, a third phase, gas, is also present in many cases. Nevertheless, these gas bubbles are considered to be part of the pore water, thus part of the liquid. Their influence can be taken into account by considering the pore fluid as more compressible than saturated water.

Understanding the physics of liquefaction requires understanding of the stress–strain behavior of the solid phase alone and both soil phases in combination as follows:

1. The behavior of dry soil, representing the solid phase alone;
2. The behavior of fully saturated and undrained soil, assuming the pore water to be completely incompressible; and
3. The behavior of nearly saturated and undrained soil, taking into account the compressibility of the pore water including some gas bubbles.

These behaviors will be discussed in the next part of this paper. The last part of this paper deals with some typical situations of liquefaction around marine structures.

Stress–Strain Behavior of Dry and Saturated Sandy Soil

Stress–Strain Behavior of Dry Soil

The stress–strain behavior of a dry sandy soil can be found by testing samples in a triaxial cell, a direct simple shear apparatus, or another test apparatus. Such a test generally yields the same results as a drained test, i.e., a test on saturated soil where the pore water can freely flow in and out of the sample and no excess pore pressure is produced.

The stress–strain response can be expressed in the stiffness tensor, which relates the stress tensor to the strain tensor. Its main components are illustrated in Fig. 1 for isotropic soils. Sand in nature and even in laboratories may not be isotropic, but the assumption of isotropy may be introduced here to clarify the most essential phenomena. The mean effective stress, σ'_{oct}, causes only the volumetric strain, ε_{vol}. The shear stress, τ, however,

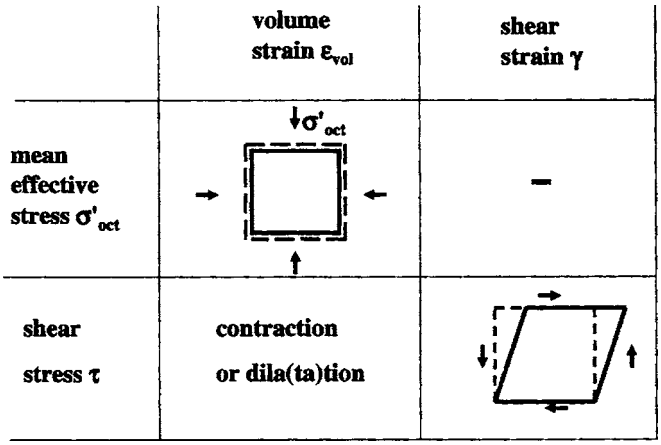

Fig. 1. Main types of stress–strain relationship

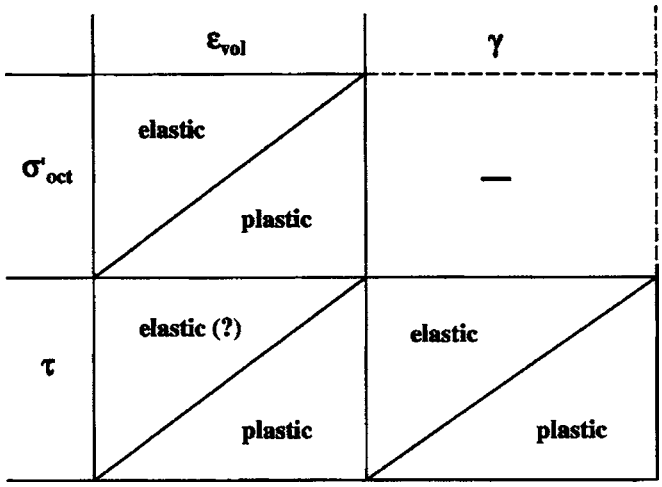

Fig. 2. Subdivision of stress–strain relationship in elastic and plastic components

causes both volumetric strain and shear strain, γ. The last type of volumetric strain is called "dilation" or "dilatation" if it is positive, i.e., if it concerns an increase in volume. It is called "contraction" if it is negative.

It should be realized that "shear stress" is only uniquely defined if the plane of the stress is indicated, e.g., the horizontal plane or the plane of the largest shear stress. In many cases, it is more practical to use the "deviator stress," i.e., the difference between the largest and the smallest principal stress, as a measure of the largest shear stress in any soil element. A similar remark can be made with respect to the shear strain.

If a soil element is loaded for the first time to a certain load level ("virgin loading"), it behaves quite differently from when it is loaded for the second time to the same load level ("reloading"). The stress–strain path with reloading does not differ much from the path with "unloading" in most cases. A rearrangement of grains with respect to each other takes place during virgin loading, which can be considered to be plastic deformation. Much less rearrangement occurs with unloading or reloading. Then the soil behaves nearly elastically.

Thus, in many cases it is justified to model the soil such that the strain tensor can be decomposed into a plastic part and an elastic part during virgin loading, whereas it consists of just an elastic part during unloading and reloading. This yields six important components of the stiffness tensor during virgin loading, as illustrated in Fig. 2. Contraction and dilation are often considered to be purely plastic. Then only five components would be relevant during loading and two during unloading. This may be justified in many cases, but not always, as will be discussed below under "Volume Strain with Monotonic Shear."

Volume Strain with Change in Mean Effective Stress

Isotropic compression and decompression can be performed in a triaxial apparatus. A typical test result is shown in Fig. 3. The negative volume strain (reduction in volume) during virgin loading can be five times the deformation during unloading or reloading. Then, the deformation during virgin loading is 80% plastic and 20% elastic.

The elastic compression modulus (or "bulk modulus") of skeleton, K, is the gradient of the line for elastic unloading/reloading. The stiffness of the soil skeleton, thus K, increases with the increase in mean effective stress when the grains are pressed upon each other. $K(\sigma'_{oct}=0)$, indicated in Fig. 3, is the value for $\sigma'_{oct}=0$. Experimental determination of this value is very difficult. In normal geotechnical practice the following can be assumed

$$K = K_{ref}(\sigma'_{oct}\sigma'_{ref})^{y}$$

where σ'_{ref}=reference stress; K_{ref}=corresponding value of K; and $y \approx 0.5$. This approximation would yield $K(\sigma'_{oct}=0)=0$, which is no problem in most geotechnical applications, but may yield wrong conclusions for some special cases of liquefaction around marine structures, as will be discussed below.

Like the elastic modulus, the stiffness in virgin loading, K_{VIRGIN}, increases with increasing mean effective stress.

Very similar results are found from oedometer tests, where the sample is restrained in all horizontal directions and only vertical deformation can occur. The gradient of the line for virgin loading is usually indicated with M or with $E_{OED}=d\sigma'_v/d\varepsilon_v$(virgin). The letter E, however, has nothing to do with "elasticity modulus," as E_{OED} is mainly referring to plastic deformation. Much larger stiffnesses are found for unloading/reloading. The gradient of the line can be expressed as $(K+4G/3)=d\sigma'_v/d\varepsilon_v(\text{unload/reload})=1/\alpha$,

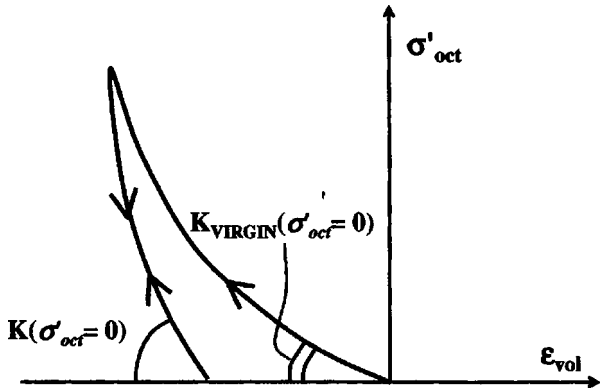

Fig. 3. Typical volume strain with isotropic compression and decompression

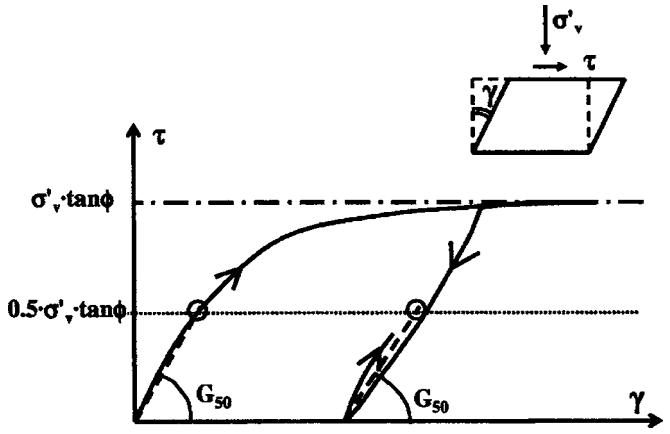

Fig. 4. Shear strain with change in shear stress

where G is the shear modulus and α is the elastic compressibility for horizontally restrained deformation. In normal geotechnical practice the E_{OED} and $(K+4G/3)$ may be assumed to be proportional to the logarithm of the (vertical) stress or the square root of the stress. These approximations do also yield zero stiffness at zero stress.

Shear Strain with Change in Shear Stress

The most commonly used instrument for shear tests of samples is the triaxial apparatus. An alternative is the "direct simple shear apparatus," in which certain interesting components of the shear stress and the shear strain are more directly imposed and measured than in a triaxial apparatus. Only the results reached with a direct simple shear apparatus are discussed in this paper. A typical result of such test is shown in Fig. 4, where τ is the shear stress in the horizontal plane, γ is the shear strain as indicated in the figure, σ'_v is the vertical effective stress, and ϕ is the friction angle, at least the friction angle as found in this way. The response is mainly elastic at relative low shear stress values—say $\tau/\sigma'_v < 0.5 \tan \phi$—and can be characterized by the shear modulus for 50% of the failure load, G_{50}. A permanent shear deformation results after shear at higher relative shear stress, whereas the shear deformation during unloading and reloading can be considered to be approximately elastic.

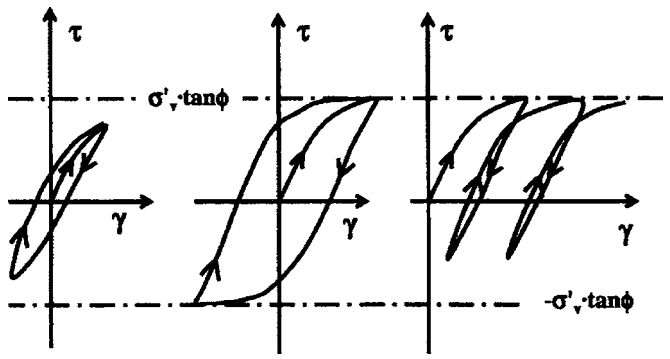

Fig. 5. Shear strain against cyclic shear stress

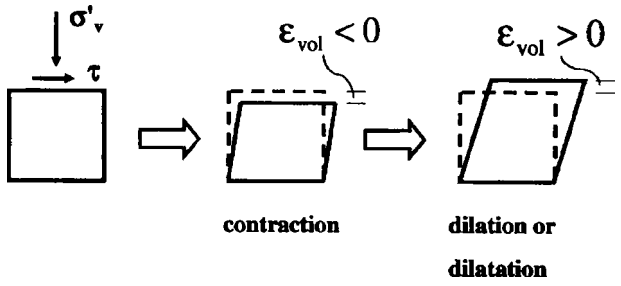

Fig. 6. Volume strain with shear test on dry sand or silt

Fig. 4 makes clear that the relative shear stress, τ/σ'_v, rather than the absolute value of the shear stress, τ, determines the shear strain. Nevertheless, the absolute values of both stresses have also some influence: like the compression modulus, the shear modulus increases with increasing mean effective stress.

Fig. 4 shows a result for such shearing that the shear stress in the initially chosen direction is always positive. Fig. 5 shows what subsequently happens if the direction of the shearing changes to "negative" and is continued to cyclic loading. Nearly elastic deformation occurs if the absolute value of the shear stress peak remains limited. Significant plastic deformation occurs with each cycle if the peak shear stress comes (close) to the failure limit. In case of asymmetric loading the permanent shear strain increases every cycle. It needs to be kept in mind that neither stress nor strain is uniform in a practical realization of the idealized test in Fig. 4.

Volume Strain with Monotonic Shear

The tests used to find the shear strain also show another feature: volume strain. Usually monotonic shearing, i.e., shearing that increases always in the same direction, yields first some contraction, i.e., volume decrease by shearing, then dilation, i.e., volume increase by shearing (see Figs. 6 and 7).

Fig. 8 illustrates a typical outcome of a monotonic direct simple shear test on medium dense sand for constant value of σ'_v. The two graphs at the left are equal, though turned 90° to show the correspondence with the other graphs. Many geotechnical applications allow for a simplification of the $\varepsilon_{vol}-\gamma$ curve by a straight line through the origin with the dilation angle, ψ, as direction coefficient. This simplification, however, is not justified for liquefaction. Important for liquefaction is the characteristic point with the smallest volume of the grain skeleton, where the phase transformation occurs, i.e., where contraction turns into dilation. It is indicated by **o** in the graphs.

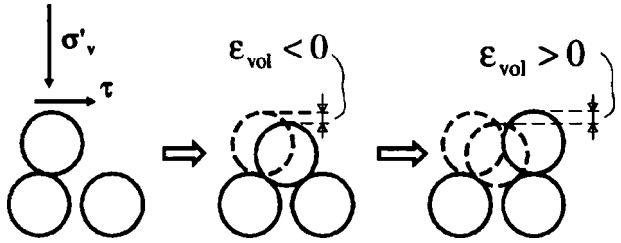

Fig. 7. Contraction and dilation by rearrangement of grains

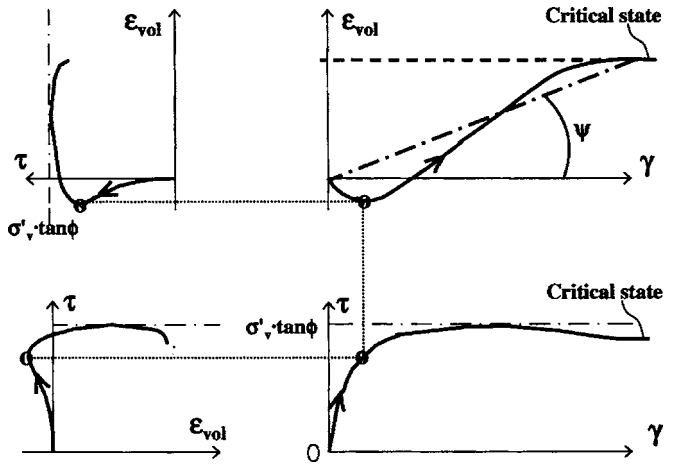

Fig. 8. Volume strain as function of shear strain and shear stress in monotonic shear of dry sand or silt

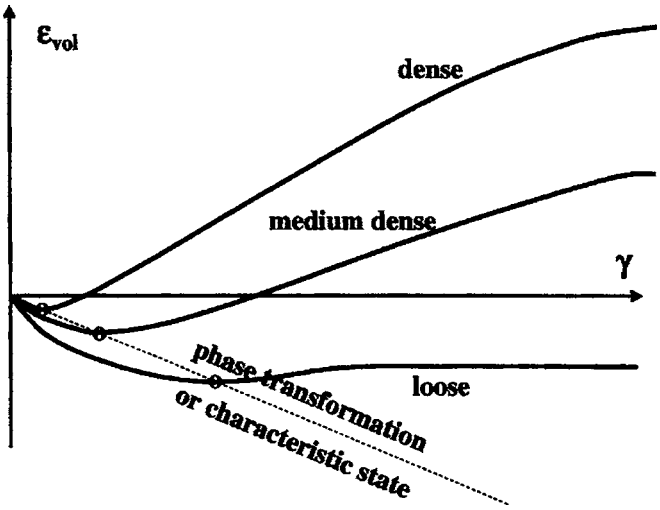

Fig. 10. Influence of density in dry monotonic shear

This point always occurs at more or less the same ratio between shear stress and normal stress: $\tau/\sigma'_v \approx \tan 28° - \tan 30°$ for all types of quartz sand and for all relative densities. The corresponding line(s) in the $\tau - \sigma'_v$ plane separate(s) the contractive region from the dilative region (Fig. 9). It is called the phase-transformation line (Ishihara et al. 1975) or characteristic line (Luong 1980a,b).

The vertical line in Fig. 9 indicates the stress path for constant σ'_v, the strains of which are illustrated in Fig. 8, until the maximum shear stress, $\tau = \sigma'_v \tan\phi$, is reached at the failure line. The shear stress slightly decreases if shearing in one way is subsequently continued (Fig. 8). If this shearing is continued long enough, dilation ends and a maximum volume is reached. This volume remains more or less constant when shearing goes on with the same velocity, whereas σ'_v and τ remain constant as well. This state of constant volume, constant shear strain rate (=shear deformation velocity), and constant stresses is called the critical state.

The degree of contraction and the degree of dilation largely depend on the relative density, defined by the density index I_D (Notation), in the initial state. Its influence is illustrated in Fig. 10. The points of minimum volume can be connected by another phase-transformation line, which is also more or less straight. The volume strain on the vertical axis starts from the initial void ratio. Fig. 11 shows the same results. Now, however, the strain is replaced with the absolute value of the void ratio. The three curves show a consequence of the theory that, before a grain skeleton reaches the critical state, deformation is so strong that any loading and deformation "history" is "erased," once it has reached this state. Consequently, each sand has, for each value of the mean effective stress, one unique critical state void ratio at which constant shearing occurs.

The influence of density can also be illustrated in graphs similar to the lower ones of Fig. 8: the looser the sand, the smaller the difference between ϕ and the angle of 28–30°, corresponding to the characteristic point. The looser the sand, the smaller the dilative zone indicated in Fig. 9.

The relative shear stress, τ/σ'_v, rather than the absolute value of the shear stress, τ, determines the volume strain, just like with the shear strain. And also here the absolute value of the vertical effective stress has some influence: the larger the effective vertical stress the more contraction for the same initial void ratio and the lower the critical state void ratio. Thus an increase in σ'_v, yields a similar effect as a decrease in density index I_D.

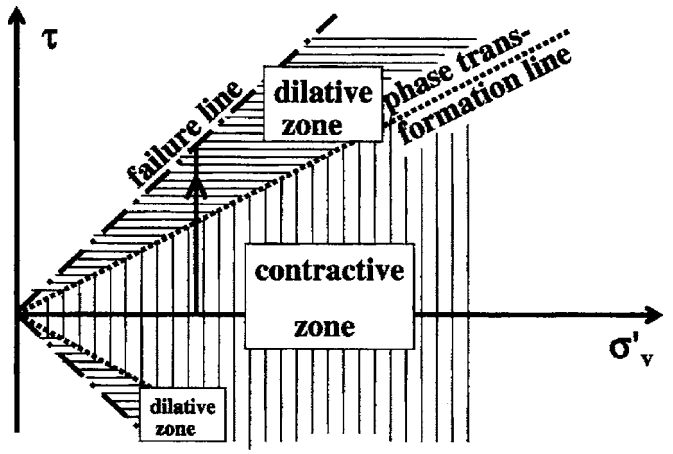

Fig. 9. Phase transformation line or characteristic line separating contractive zone from dilative zone in $\tau - \sigma'_v$ plane

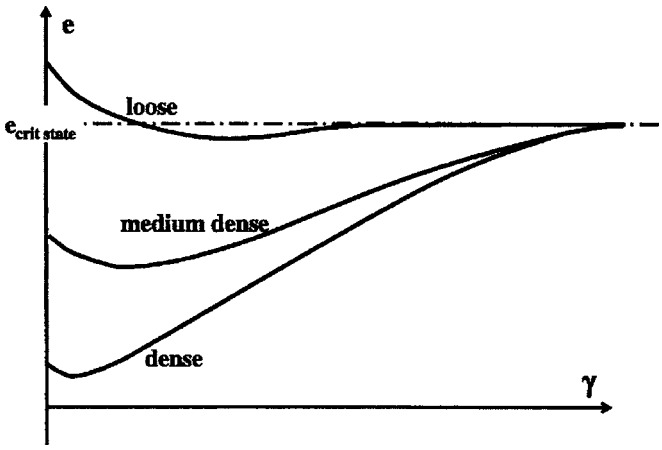

Fig. 11. Influence of density in dry monotonic shear: unique void ratio after much shearing

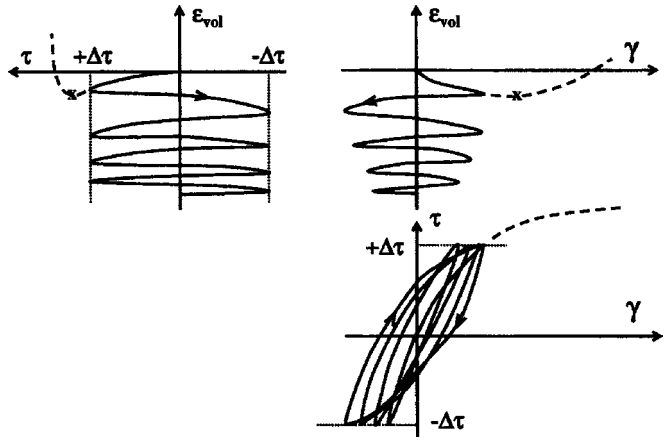

Fig. 12. Volume strain with moderate cyclic shear loading of dry sand or silt

Volume Strain with Cyclic Shear

Densification of sandy soil is nearly always a result of cyclic shearing. A typical result is shown with solid lines in Fig. 12. The $\tau-\gamma$ curve corresponds to the left part of Fig. 5. Fig. 13 illustrates the influence on volume strain of relative density; Fig. 14 the influence on volume strain of shear stress amplitude relative to the vertical (effective) stress, $\Delta\tau/\sigma_v'$. Tests with imposed shear strain amplitude show similar tendencies.

Dilation does not seem to play a role in most cases of cyclic shearing, but experience shows that severe vibration can induce loosening. Fig. 15 shows the possible behavior of (medium) dense sand in case of cyclic shearing at such high amplitude that, twice during each cycle, the maximum shear stress is reached and significant plastic shear strain occurs as illustrated in the middle part of Fig. 5: the dilation appears to be partly elastic. After one or two cycles, a kind of equilibrium is reached in which the same cycle is followed each time and contraction in one part of each cycle is compensated for by dilation in the other part.

Such equilibrium is also possible with moderate shear amplitude in the case of asymmetric loading, i.e., shear loading with nonzero average shear stress. See the right part of Fig. 15. Consequences will be discussed under "Undrained Response to Cyclic Shear" and are illustrated in Figs. 24 and 25.

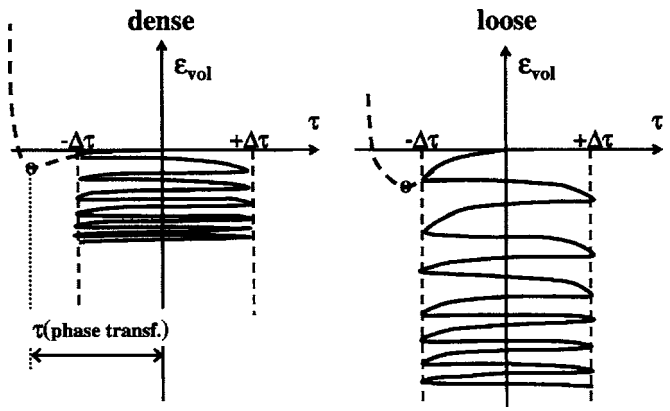

Fig. 13. Influence of density on volume strain in dry cyclic shear

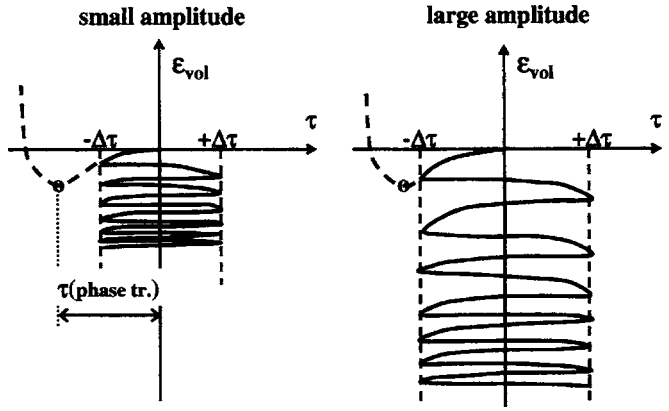

Fig. 14. Influence of stress amplitude on volume strain in dry cyclic shear

Stress–Strain Behavior of Completely Undrained Saturated Soil

Tests on samples of dry or fully drained sandy soil can be used to find the above constitutive properties. Completely undrained tests, however, are more common to determine the behavior and constitutive properties, relevant for liquefaction. Geotechnical engineers apply the terms "completely undrained" or just "undrained" for the situation characterized by two important limiting cases:

- The soil is completely saturated with water; no gas is present in the pore fluid; and
- No drainage occurs.

The main consequence for the stress–strain behavior is that the volume strain is almost zero, as pure water can be assumed as incompressible. Volume strain is no longer an interesting output variable of such tests, whereas the development of pore pressure is a new interesting output variable. Also the stress path, i.e., the relationship between the different components of the effective stress, is an interesting result of an undrained test, whereas it is usually imposed in dry tests.

If the soil is contractive an increase of pore pressure is to be expected during undrained shear, as explained in the next paragraph. The increase may yield partial liquefaction or complete liquefaction, as defined in the "Introduction."

The result of an undrained test can, in principle, be predicted by superposition of the results of two types of dry tests: dry shear

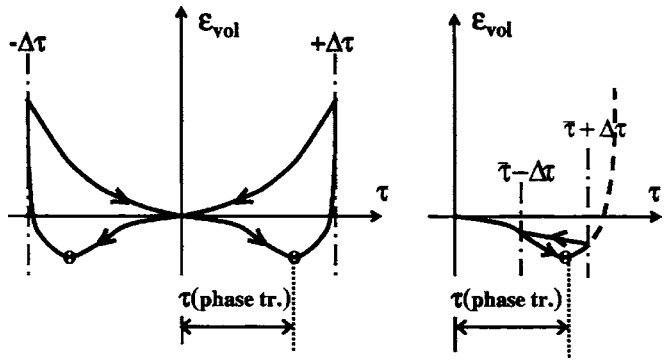

Fig. 15. No net volume strain in dry cyclic shear due to alternating contraction and dilation with very large amplitude or strongly asymmetric load

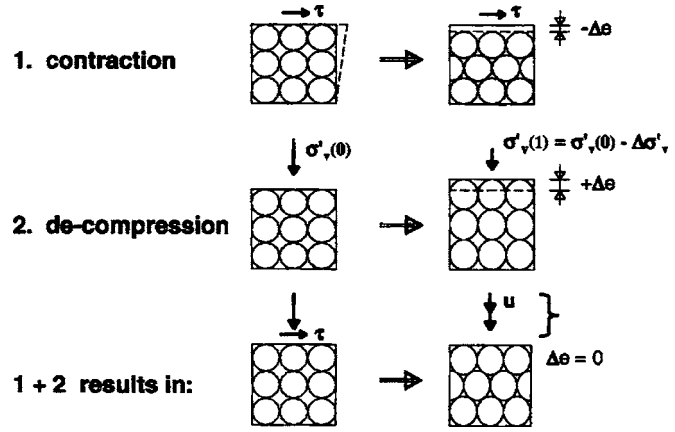

Fig. 16. Undrained response to shear as superposition of dry shear and dry decompression

tests and dry isotropic decompression tests, as illustrated in Fig. 16 for horizontally restrained tests. The indices 0 and 1, in Fig. 16 refer to the situation before and after loading, respectively. The decrease in void ratio $-\Delta e$ found from the shear tests should be compensated for by the increase $+\Delta e$ found from the last type of tests, yielding a certain decrease in effective vertical stress. The absolute value of this decrease equals the increase in pore pressure, if the total vertical stress, σ_v, is kept constant.

Undrained Response to Monotonic Shear

Typical results of monotonic undrained triaxial shear tests can be found in Ishihara (1993). Here, corresponding results will be shown for direct simple shear tests. A typical result for medium dense sand is presented in Fig. 17. According to the usual procedure, the shear stress gradually increases, whereas the total vertical stress is kept constant. The effective vertical stress, however, is not constant. Its variation is shown, jointly with the shear stress variation, as stress path in the left graph. The excess pore pressure, u, can be found in this graph as the difference between effective vertical stress and total vertical stress, which is equal to the initial vertical effective stress.

The stress path in this graph shows how the effective vertical stress is first reduced by the contraction induced excess pore pressure and then increased by the dilation induced "suction," i.e., negative excess pore pressure. The effective stress becomes even much larger than the total stress. Thus, the shear stress can also rise far above the shear stress in an undrained test. Compare the right graph with the corresponding graph of Fig. 4.

The point of minimum vertical effective stress and maximum excess pore pressure corresponds to the phase transformation point in drained loading. A more or less constant shear stress is reached after a lot of shearing, as shown in the right graph. This stress is called the steady state shear stress or steady state shear strength (Castro 1975). It corresponds to the end point of the stress path shown in the left graph. This point lies on the failure line with $\sigma_v' = \tau / \tan \phi$, which means that also the normal effective stress is constant during this shearing and the conclusion is justified that this steady state of constant volume, constant effective stresses, and continuing shearing must be the same as the critical state. This state is reached here by a change in vertical effective stress, whereas it is reached in dry tests with constant vertical stress by a change in void ratio.

The influence of density is illustrated in Fig. 18. The graphs show that the steady or critical state shear stress is very high for dense sand: out of the range of this graph. It also shows that the steady state of the loose sand, unlike the one for medium dense sand, is reached by a decrease in effective stress: the end of the loose curve in the left graph indicates a lower value of σ_v' than the beginning of the curve along the σ_v' axis. Complete liquefaction occurs with very loose sand after enough shearing: the steady state shear stress is practically zero.

When the test illustrated in Fig. 17 is repeated with the same density index, however starting with a higher value of σ_v', much higher relative pore pressures are induced. Then, the shapes of the curves approach the ones for loose in Fig. 18 more instead of the medium ones. This higher relative pore pressure corresponds to the increase in contraction with increase in effective stress, found with dry tests. The pore pressures increase such that, according to the theory of steady or critical state stress and confirmed by many experiments, a stress path with the same end point as the first test is found. Thus, the steady or critical state shear stress is only a function of the density or void ratio. This function can also be considered to be the steady or critical state void ratio as a function of shear stress. The functions of the steady state void ratio against the vertical effective stress or mean effective stress are very similar. Experience shows that these functions usually have the shape of a straight line in a semilogarithmic plot, as illustrated in Fig. 19. The line is often called the steady state line or critical state line. Different types of soil yield different steady state lines.

No liquefaction (due to monotonic loading) can occur if the void ratio and shear stress of a sand element correspond to a point below the steady or critical state line, as the shear stress of this element is lower than the steady or critical state shear strength. It is often stated that a sand element above the steady state line is sensitive to liquefaction. This is a conservative approach. Such sand elements have an undrained stress path and τ/γ curve as indicated in Fig. 18 for loose and very loose sand. The shear stress according to this path has a first maximum, indicated with a star in the curve. It is reached after a relatively limited shearing of $\gamma \approx 2-5\%$.

No liquefaction will occur as long as the shear stress is lower than the shear stress of the instability point, even if it is higher than the steady or critical state shear strength. This maximum can be considered to be an instability point: any further shearing yields a reduction of the shear strength. If all surrounding elements are in a similar state and if the shear load is constant, any sudden small deformation or loading yields a sudden collapse of the soil mass, as no equilibrium is possible any more or only after a lot of shear strain. This type of behavior is characteristic for liquefaction flow slides and other cases of liquefaction due to monotonic loading (Stoutjesdijk et al. 1998). Such liquefaction is not typical for marine structures and will not be discussed here any further.

Undrained Response to Cyclic Shear

A typical stress path and shear stress–shear strain curve for undrained cyclic simple shear loading are shown in Fig. 20. The corresponding pore pressure development is shown in Fig. 21. An important test result is the number of cycles to liquefaction, N_L. More detailed observation shows that the increase in pore pressure per cycle is usually relatively strong in the beginning. This corresponds to the relatively large contraction during the first cycles in a drained test as sketched in Fig. 12.

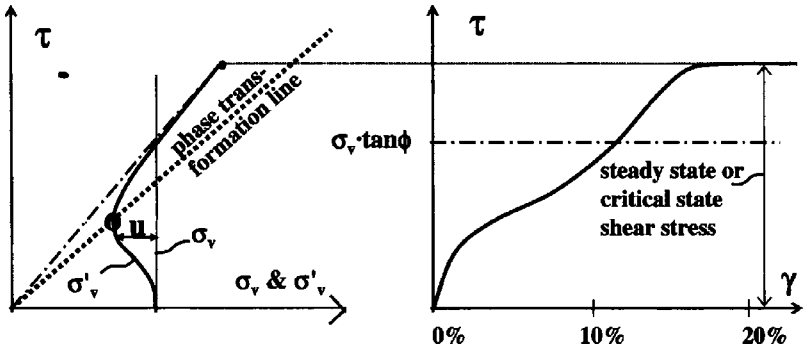

Fig. 17. Typical behavior with undrained monotonic shear

It is also large at the end due to the relatively large pore pressure and consequent large relative effective shear stress amplitude, $\Delta\tau/\sigma'_v$. This also causes a significant increase in shear strain amplitude and a reduction in the (apparent) shear stiffness.

It should be noted that the sketched behavior belongs to tests with constant shear stress amplitude $\Delta\tau$. Tests with constant shear strain amplitude, $\Delta\gamma$, are also performed occasionally. Such tests show a reduction of the shear stress amplitude and a much more gradual increase in pore pressure at the end.

The two main parameters influencing the contraction in drained tests are I_D and $\Delta\tau/\sigma'_v$, as shown in Figs. 13 and 14. Correspondingly, the number of cycles to liquefaction, N_L, shown in Fig. 21, is mainly a function of these two parameters, provided $\Delta\tau/\sigma'_v$ is replaced with the cyclic shear stress ratio (CSSR)$=\Delta\tau/\sigma'_{v0}$, where σ'_{v0} is the initial vertical (effective) stress. Typical curves are shown in Fig. 22. Another parameter with a significant influence is the stress level: increasing σ'_{v0} alone, while keeping CSSR constant, causes a decrease in the value of N_L, corresponding to the increase in contraction with increase in vertical effective stress in dry tests. Other factors of (secondary) influence are:

1. Aging in natural soils;
2. Sampling technique (e.g., freezing) and/or the sample preparation techniques (air pluviation, vibration, moist tamping etc.) in the laboratory; and
3. Preshearing, i.e., the application of some cyclic loading to the sample and subsequent drainage before the initial density is determined and the actual test is performed.

All these factors influence the structure of the skeleton in such a way that two tests on the same sand at the same initial density under exactly the same loading may behave differently.

According to some researchers, complete liquefaction is reached even in very dense sand. According to others, equilibrium with no more than partial liquefaction seems possible, as illustrated in Fig. 23. Cycling around the equilibrium point means an alternating process of increasing pore pressure when the shear stress decreases and a decreasing pore pressure when the shear stress increases. This corresponds to a process of alternating contraction and dilation with very large amplitude, as indicated in Fig. 15.

All these curves refer to tests with symmetrical loading: a shear stress varying around zero average. The question about reaching complete liquefaction or reaching no more than partial liquefaction is clearer with asymmetric loading. No complete liquefaction is reached if the average relative shear stress is sufficiently large and the relative shear stress amplitude is sufficiently small, unless the sand is (very) loose. Instead equilibrium with constant average pore pressure is reached after sufficient cycles. The equilibrium point in the stress path is laying at the intersection of the average shear stress and the phase transformation line (Vaid and Chern 1983; Ibsen 1994), as illustrated in Fig. 24 and the upper curve in Fig. 26. If the starting point lies between this line and the failure line, i.e., if the average shear stress is high enough and the sand is not too loose, the average pore pressure becomes negative and the effective stress increases, as illustrated in Fig. 25 and the lower curve in Fig. 26.

The word "equilibrium" is partly misleading: the mean pore pressure may not change during the final load cycles, the shear strain often continues, as illustrated in the right parts of the Figs. 24 and 25. This is called "cyclic mobility" (Castro 1975).

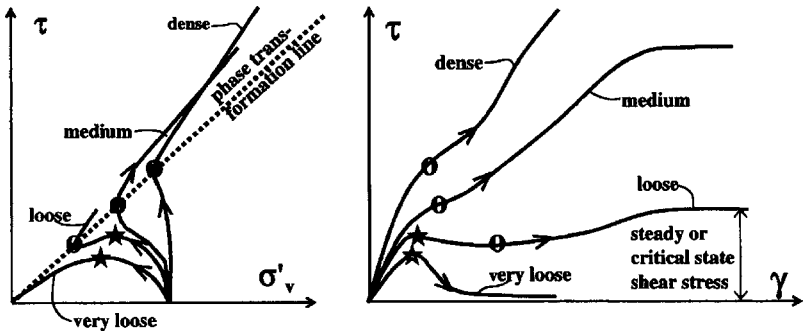

Fig. 18. Influence of density in undrained monotonic shear

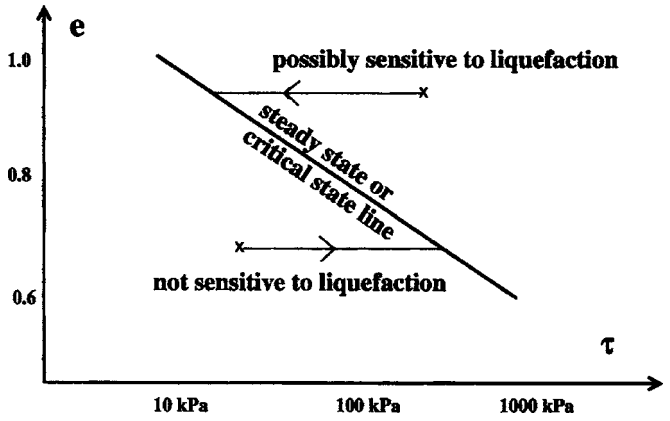

Fig. 19. Steady state or critical state shear stress as function of void ratio

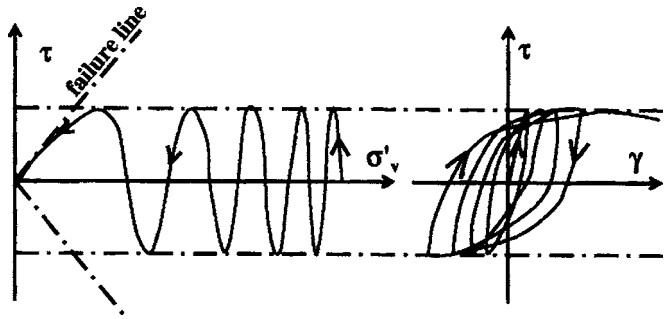

Fig. 20. Effective stresses and shear strains with undrained cyclic shear

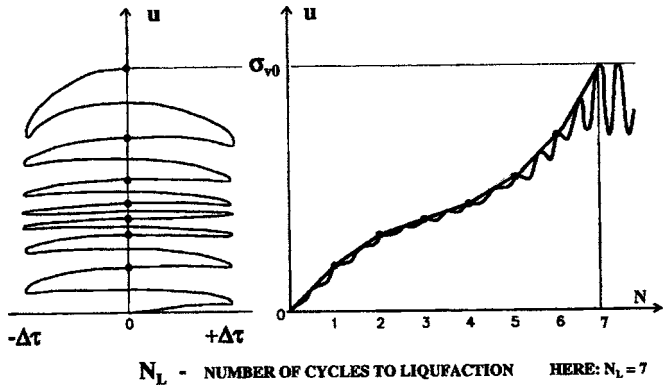

Fig. 21. Residual excess pore pressures in undrained, cyclic shear

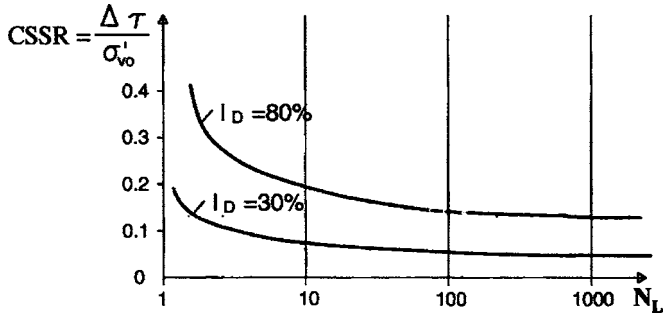

Fig. 22. Influence of cyclic shear stress ratio and density index on number of cycles to liquefaction in undrained cyclic shear

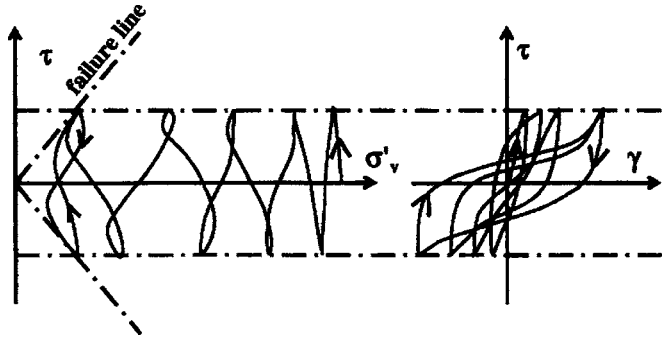

Fig. 23. Stresses and strains in dense sand with large amplitude undrained cyclic shear

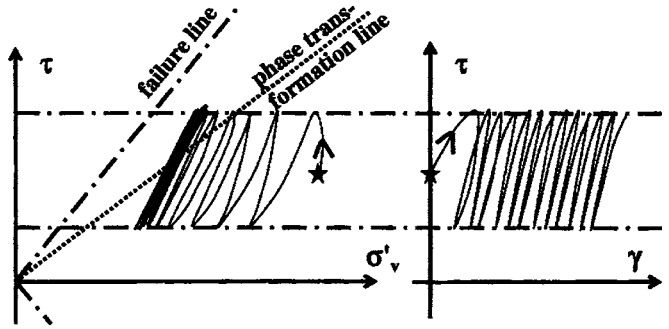

Fig. 24. Stresses and strains in dense sand with asymmetric undrained cyclic shear: partial liquefaction and cyclic mobility

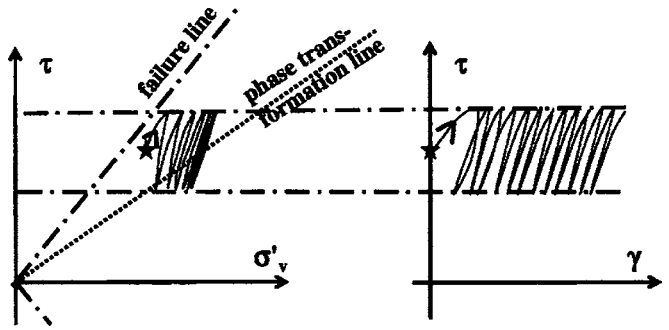

Fig. 25. Stresses and strains in dense sand with very asymmetric undrained cyclic shear: negative excess pore pressure and cyclic mobility

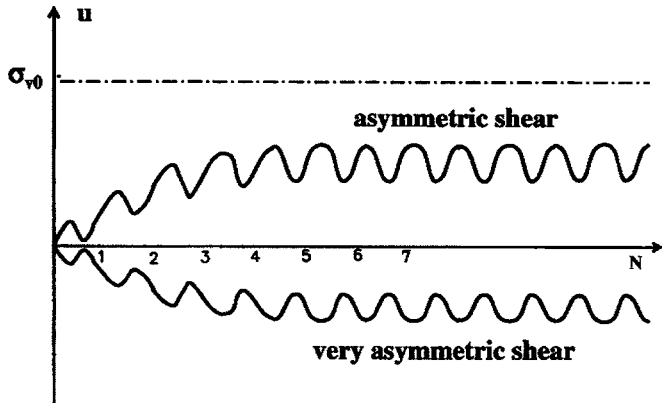

Fig. 26. Pore pressure development in dense sand with (very) asymmetric undrained cyclic shear

Influence of Pore Fluid Compressibility

The compressibility of completely saturated water is negligible compared to the compressibility of the soil skeleton only. The pore fluid compressibility, β, and the compression stiffness of the pore fluid, $K_w = 1/\beta$, directly follow from the content of free (nonsolved) gas and the absolute water pressure. K_w is nearly equal to the absolute pressure divided by the gas content. Thus, at 10 m below mean sea level, where the absolute pressure equals approximately 0.2 MPa, pore water with 1% of gas will have $K_w \approx 0.2/0.01 = 20$ MPa.

This means that the compressibility of the pore fluid may have the same order of magnitude as the compressibility of the soil skeleton. It cannot be neglected for many types of liquefaction, if the gas content is more than 0.3%. Not much is known about the gas content in sandy seabeds. There are good reasons to assume, however, that the gas content is often larger than 0.3% (see Sandven et al. 2005).

Compressibility of the pore water allows for some decrease in skeleton volume as soon as the soil has the tendency to contract, even without any drainage. It causes less increase in pore pressure, less decrease in effective stress, and less decrease in shear strength. In case of a tendency to dilate or in case of a decrease in total stress, compressibility of the pore water causes less decrease in pore pressure and less increase in effective stress and shear strength.

The behavior of such soil if no drainage is possible can generally be considered as being in between the behavior of completely dry or drained soil, and the behavior of completely saturated, undrained soil.

Typical Situations of Liquefaction around Marine Structures

A few typical situations of liquefaction around marine structures are briefly described below. Where relevant, reference will be made to similar situations discussed in the following papers in this issue and the next issue.

Liquefaction due to monotonic loading will not be discussed here: only liquefaction due to fluctuating loads, either caused by waves or by an earthquake. Complete liquefaction and partial liquefaction will both be discussed. The focus will be first on situations where the liquefaction concerns "instantaneous" pore pressures; later to those with residual excess pore pressures. Instantaneous or momentary pore pressures are fluctuating with the load, but not necessarily in phase with the load. They are probably dominated by elastic soil behavior. Residual pore pressures are gradually increasing or decreasing and are mainly due to plastic deformation of the soil skeleton in most cases. The term residual is slightly misleading, as positive residual excess pore pressures usually disappear sooner or later thanks to drainage.

Wave Induced Instantaneous Pore Pressures in Seabed

A brief account of instantaneous pore pressure in seabed is given in sections 10.1.2 and 10.4 of Sumer and Fredsøe (2002). The pore pressure distribution in a sandy seabed with incompressible pore water is a quasistationary one: At each moment it is completely determined by the pressure distribution along the soil boundaries at that moment and the flow resistance distribution in the soil. All pressure fluctuations occur simultaneously: there is no phase shift.

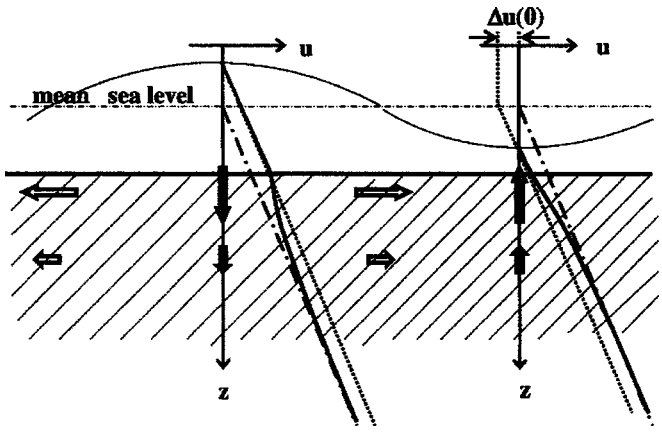

Fig. 27. Instantaneous pore pressures and pore flow under waves with incompressible pore fluid

In the special case of a sinusoidal wave with wavelength, L, over a horizontal bed and homogeneous soil the absolute value of the excess pore pressure decreases with depth, z, according to $\exp(-z/z_1)$, where $z_1 = L/2\pi$ (Yamamoto et al. 1987; Verruijt 1982). See Fig. 27. The value of z_1 characterizes the damping of pore pressure amplitude with depth in case of incompressible pore water. Water flows into the soil underneath the crest and the same amount of water flows out of the soil underneath the trough. In between the pore flow is typically horizontal. Half a wave period later, the flow is reversed everywhere.

The excess pore pressures are largest underneath the wave crest and lowest underneath the wave trough, according to the definition of "excess" with mean sea level as reference. Nevertheless the effective stresses are also largest underneath the wave crest and smallest underneath the wave trough, yielding the highest liquefaction risk underneath the trough. The reduction of the effective stresses underneath the wave trough, however, is too small to cause complete instantaneous liquefaction, even just underneath the seabed. This follows from the limitation of the wave steepness, which is such that the amplitude of the pressure head fluctuation at the seabed, $\Delta u(0)/\rho_w g$, is always much smaller than z_1.

The effective stress fluctuations, however, are large enough to cause residual excess pore pressures in many cases. A conservative approximation yields the following fluctuations just underneath the seabed, where $z \ll z_1$, in case of a progressive, sinusoidal wave. The maximum vertical effective stress underneath the crest $= +\Delta u(0) \cdot z/z_1$. The minimum, during wave trough $= -\Delta u(0) \cdot z/z_1$. No shear stresses occur in the horizontal and vertical planes at these moments, which means that the direction of the first principal stress is vertical during the wave crest and may be horizontal or vertical during the wave trough. Halfway in between the crest and trough, at the moment of maximum horizontal pressure gradient, i, along the seabed, the situation is completely different (Fig. 28). The pore pressure gradient is completely horizontal, yielding no pore pressure induced vertical effective stress, but a maximum of the shear stress in a horizontal plane, τ_{zx}. This maximum equals $[\tau_{zx}]_{max} = \rho_w g z i = \Delta u(0) \cdot z/z_1$ according to linear wave theory, thus the same value as the vertical effective stress amplitude. Half a wave period later, the opposite value is found: $[\tau_{zx}]_{min} = -\Delta u(0) \cdot z/z_1$. The principal

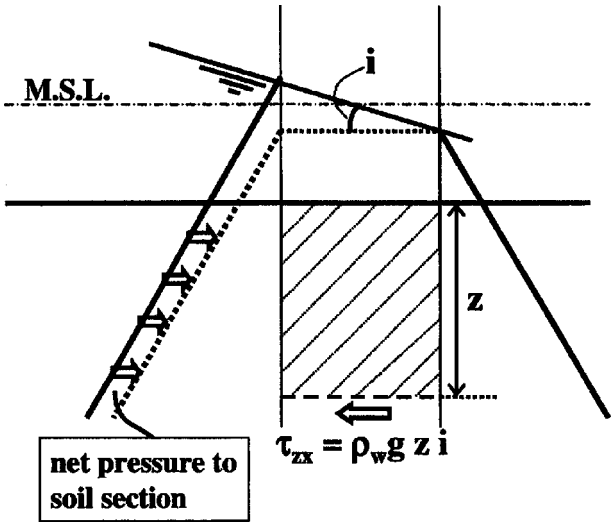

Fig. 28. Approximation of instantaneous pore pressures under wave halfway crest and trough with incompressible pore fluid

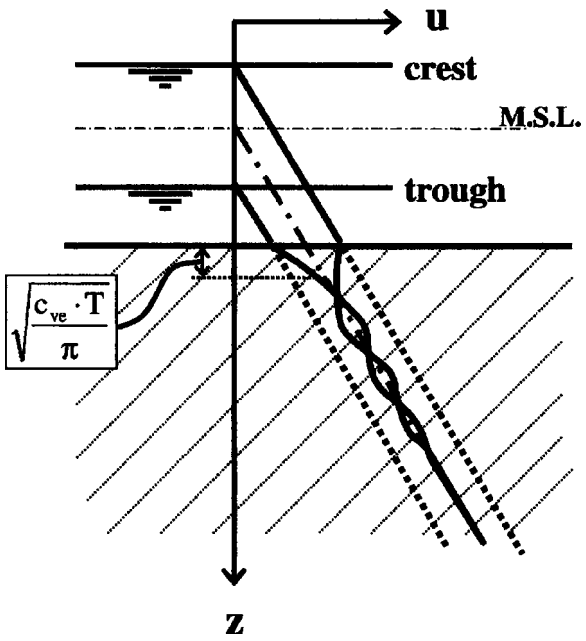

Fig. 29. Instantaneous pore pressures under waves in seabed with compressible pore fluid

stresses clearly rotate. The stress fluctuation cannot be simulated either in a direct simple shear test or in a triaxial test.

With some gas in the pores the pore water is compressible and a completely different picture may occur, (e.g., Yamamoto et al. 1978; Verruijt 1982). The consequent pore-water compressibility allows for storage of some pore water in the soil during increasing pore pressure; pore water that leaves those again when the pressure decreases to its original value. Thus, the pore water flowing down into the soil during the wave crest does not come as deep as it would with incompressible pore water. The damping of pore pressure amplitude with depth is stronger. There is also a phase shift and the pressure distribution depends not only on the actual loading but also on the past loading.

The amplitude of the pore pressure fluctuation reduces quickly with depth underneath the seabed if the pore water compressibility, β, is much larger than the (elastic) skeleton compressibility, α (Fig. 29). Assuming linear elastic, homogeneous soil, yields a variation approximately according to $\exp(-z/z_2)$ with $z_2=\sqrt{(c_{ve}T/\pi)}$, where T is the wave period and c_{ve} is the consolidation coefficient for elastic, horizontally constrained (de)compression: $c_{ve}=k/[\gamma_w(\alpha+n\beta)]\approx k/(\gamma_w n\beta)$. The parameter z_2 is the characteristic length for pore pressure amplitude damping due to elastic storage. In many cases $z_2 \ll z_1$. For example, if $T=10$ s, the water depth=10 m, $k=10^{-5}$ m/s, $n=0.4$, and the gas content is 1%, then $\beta=1/(20\ \text{MPa})$, $c_{ve}=0.05\ \text{m}^2/\text{s}$, $z_1=15$ m, and $z_2\approx 0.4$ m. At a depth of $3z_2$ hardly any pore pressure fluctuation occurs: the water fluctuation at the soil surface is nearly completely transferred to stress fluctuation in the much stiffer skeleton.

This also means that large vertical pore pressure gradients occur in a relatively small top layer of the soil. The amplitude of these gradients $\approx \Delta u(0)/z_2$, where $\Delta u(0)$ is the amplitude of the water pressure fluctuation at the seabed surface. During wave trough, complete liquefaction may occur (Fig. 30) if $z_2\approx\Delta u(0)/(\gamma_w)$, as has been proven by Zen and Yamazaki (1990a,b, 1991) in their extensive study including laboratory tests, field measurements, and theoretical analyses. Such complete liquefaction may also have occurred near the edges of the block houses in Capbreton, as discussed in Mory et al. (2006).

Wave Induced Instantaneous Pore Pressures underneath Impermeable Floor

The total stress fluctuations caused by waves over an uncovered seabed consist completely of water pressure fluctuations: the effective stress at the sand surface is and remains zero. However, the stress fluctuations underneath an oscillating caisson, such as those at the harbor side of a caisson breakwater, usually consist largely of effective stress fluctuations. This situation could be compared to the theoretical case sketched in Fig. 31, where a cyclic fluctuating vertical load is transferred through a concrete floor and a thin drainage layer to a sandy seabed, while the pore pressure in the drainage layer is kept constant. This situation has also been elaborated on by Verruijt (1982).

Now, the picture appears opposite to the previous one: a strong variation with depth of the pore water amplitude, if the pore water is incompressible and hardly such variation with compressible pore water. Indeed, the pore water will take over the stress fluctuation at increasing depth, if the pore water is incompressible or at least much less compressible than the soil skeleton, i.e., if $\beta \ll \alpha$. Again, the characteristic depth $z_2\approx\sqrt{(c_{ve}T/\pi)}$. Unlike the previous case, the value of c_{ve} is dominated by the skeleton

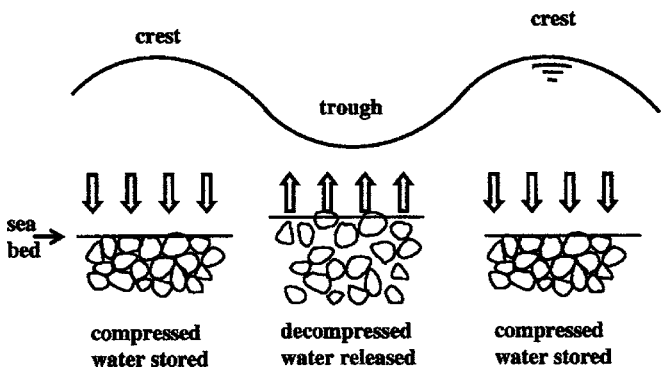

Fig. 30. Instantaneous liquefaction caused by wave

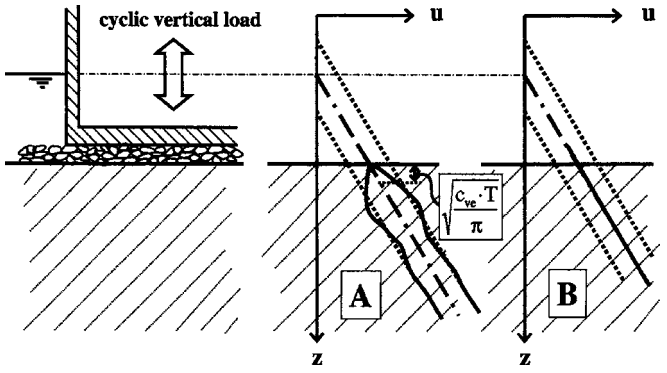

Fig. 31. Instantaneous pore pressures in seabed under cyclic loaded structure

compressibility: $c_{ve} \approx k/(\gamma_w \alpha)$. For example if $T=10$ s, $k=10^{-5}$ m/s, $\alpha=1/(50$ MPa), $c_{ve}=0.05$ m^2/s, and $z_2 \approx 0.4$ m. The right hand part of Fig. 31 shows a situation where the relatively compressible pore water does not take over the stress variation at the surface.

This phenomenon is nicely illustrated in the tests performed on a wave loaded caisson in the Large Wave Flume in Hannover (Kudella and Oumeraci 2004; Kudella et al. 2006). Significant pore pressure fluctuations were found after careful degassing of the sand. This is in great contrast to the tests performed in the same flume with a very similar setup in 1993, when some air was present in the pores of the sand and no pore pressure fluctuations were found at a depth larger than 0.3 m below the sand surface (Richwien and Perau 1999).

Negative Instantaneous Pore Pressures with Fast Shearing of Fine Dense Sand

Dredging causes relatively quick changes in soil stress. This quick, monotonic loading may yield liquefaction in slopes of loose sand. In dense sandy soil, however, the opposite may be observed, especially if the sand is fine. Cutting goes along with very large shear deformations. In undrained dense sand these large deformations go along with large negative pore pressures and are only possible if large shear stresses are mobilized, as illustrated in Fig. 18. Sand with low permeability behaves practically undrained if it is cut at large speed in relatively thick layers. Usually the cutting forces become too high and the speed and/or the layer thickness should be reduced in order to allow for the entrance of water into the pores. This process is illustrated in Fig. 32. Formulas have been developed for the calculation of the cutting forces (e.g., van Os and van Leussen 1987 or Palmer 1999). An approximate formula reads

$$\text{cutting force per unit width} = \frac{v \cdot d^2 \cdot \gamma_w \cdot \Delta n}{k}$$

where v=cutting speed; d=thickness of cut soil layer; and Δn=change in porosity required to allow for shearing. The formula is not valid anymore if the pore pressure becomes so negative that cavitation develops. This mechanism limits the cutting forces, especially in shallow water.

Another example of the effect of negative instantaneous pore pressures with fast shearing of fine sand is the reduction of the damage caused by ships sailing into the sandy banks around bridge piers, if the sand is not too loose (Ottesen Hansen 2006).

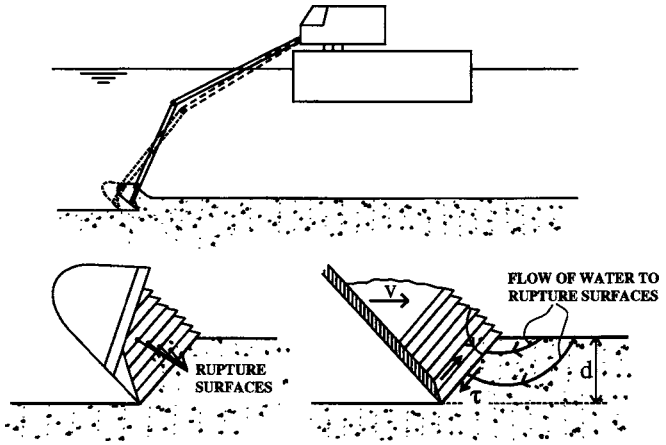

Fig. 32. Negative instantaneous excess pore pressures with cutting in fine, dense sand

The effect of negative pore pressures and increased shear strength of sand also occurs with breasting dolphins made of relatively thin vertical piles and founded in dense sand. These dolphins should be able to absorb the energy of mooring ships. Such dolphins derive most energy absorption capacity from the bending of the piles. The bending is influenced by the soil resistance, which is significantly larger during the short loading of a ship collision than during stationary loading.

The quantifying of the effect of negative pore pressures and the consequent increase in soil strength and stiffness during short duration loading is discussed in Ottesen Hansen (2006).

Earthquake Induced Residual Pore Pressures

Liquefaction of loose to medium dense sand is a well known phenomenon during earthquakes. A typical case is illustrated in Fig. 33. The cyclic horizontal movement of the rock base enforces the sand layers above it to accelerate and decelerate similarly. The acceleration goes along with horizontal shear stresses: the upward propagation of a shear wave. The shear stress in the upper sand layers is roughly proportional to the depth below the soil surface, z, just like the vertical stress, causing a relative shear stress that does not strongly vary with depth.

The loading of a sand element at depth z is very similar to the undrained symmetric cyclic loading in a direct simple shear apparatus, as illustrated in Figs. 20–22. The main difference is the irregularity of the shear loading due to the irregularity of the

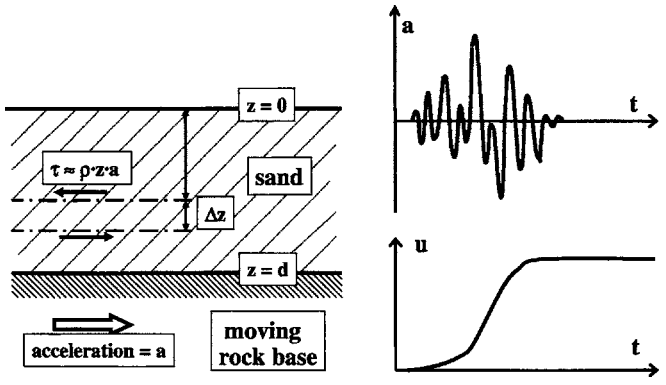

Fig. 33. Earthquake induced residual excess pore pressures

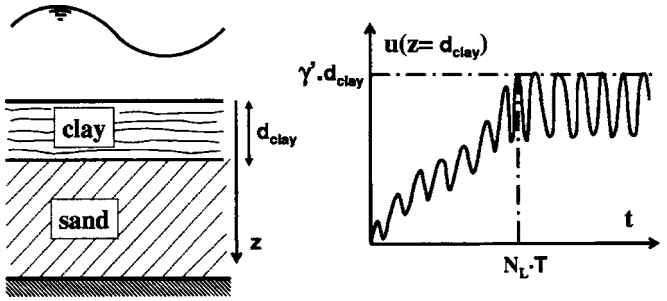

Fig. 34. Wave induced residual excess pore pressures in undrained sand layer

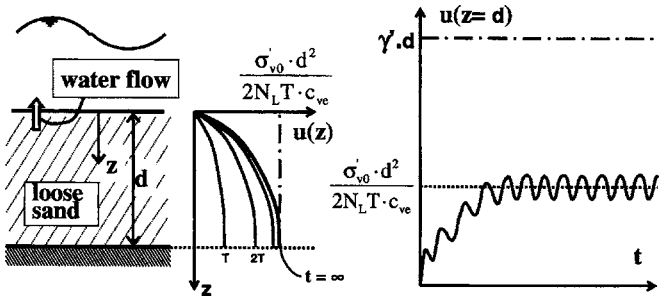

Fig. 35. Wave induced residual excess pore pressures in drained sand layer

horizontal acceleration, a. Fortunately for structure stability, the highest excess pore pressure usually occurs later than the highest acceleration loading. Thus, the moment of the smallest foundation strength usually does not coincide with the moment of the highest load. The process of pore pressure reduction due to drainage can be characterized by the "characteristic drainage period" $T_{CHAR,DRAIN}$, defined here as the time characteristic for the drainage of any excess pore pressure. It is specified in this case as $T_{CHAR,DRAIN}=d^2/c_{ve}$, which is usually much longer than the duration of the earthquake. Thus, drainage is only relevant in the case of thin layers (small value of d) or fairly permeable sand or gravel (high value of c_{ve}).

Differences among the soil layers cause, in practice, a spatial variation in shear wave propagation, in generation of excess pore pressures, and in drainage. Some effects are demonstrated in the paper presented by Sawicki and Swidzinski (2006).

Wave Induced Residual Pore Pressures

Wave loading of the seabed is different from earthquake loading in several ways:

1. The duration is much longer: many hours instead of approximately 1 min;
2. The frequency is lower: 0.1 Hz, rather than 1 Hz; and
3. The stress fluctuation is different, as explained under "Wave Induced Instantaneous Pore Pressures."

Nevertheless, the pore pressure development of a sandy soil underneath the seabed under wave loading looks similar to the one with earthquakes if drainage is prevented by a clay layer on top of the sand. The pore pressure buildup is similar to the one illustrated in Fig. 21 (see Fig. 34). Complete liquefaction may occur right underneath the clay layer.

More common is the situation of seabed sand where excess pore water can drain upward to the sand surface. Drainage is much more important than with earthquakes due to the lower load frequency and the longer duration.

The residual excess pore pressure may develop as shown in Fig. 35 in the case of a constant moderate wave load. Drainage just compensates the generation of excess pore pressures after a number of waves causing an apparently permanent situation of partial liquefaction. The time needed to reach this equilibrium is once or a few times the "characteristic drainage period" $T_{CHAR,DRAIN}$. The maximum excess pore pressure is proportional to σ'_{v0}; $T_{CHAR,DRAIN}/(N_L \cdot T)$.

The situation cannot continue forever, because the constant flow of pore water out of the soil means constant densification. The densification causes not only a settlement of the sea floor, but also an increasing resistance to the generation of pore pressure. This increase is usually more than would be expected from an increase in relative density only, such as those of which the results are presented in Fig. 22. The structure of the sand skeleton "improves" such that a slight increase in density corresponds to a large increase in resistance to liquefaction (Smits et al. 1978). The increase in resistance to liquefaction is called "history effect" or "preshearing." The characteristic time for this effect is usually longer than $T_{CHAR,DRAIN}$ (see Fig. 36).

These processes have been observed in several of the wave flume tests performed in the framework of LIMAS and before. Details can be found in Sumer et al. (1999, 2006) and Teh et al. (2003, 2004, 2006). Applications to engineering examples are described, among others, in Sawicki and Swidzinski (1989), De Groot et al. (1991), and De Groot and Meijers (1992).

A consequence of the increase in resistance to liquefaction during wave loading is that a sandy seabed does not liquefy again after a certain number of storms, unless the wave load of the later storm is higher than the loads that occurred earlier with sufficient frequency. This may not be the case in all circumstances. Very high wave loads may cause a shear loading in dense sand that brings about (instantaneous) dilatant behavior during part of the load cycle, as illustrated in Fig. 15, and a consequent situation of near liquefaction with still relatively high shear strength at high shear strain, as illustrated in Fig. 23. In contrast to Fig. 23, however, drainage occurs at the seabed surface. Nevertheless a stationary situation may occur if the dilative part of the cycle dominates the contractive part, such that sufficient water is sucked in to compensate for the drained water (see Teh et al. 2004, 2006).

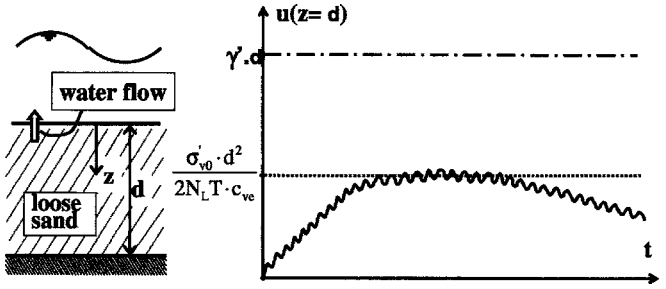

Fig. 36. Densification and history effect or preshearing effect with wave induced residual excess pore pressures in drained sand layer

Excess Pore Pressures around Wave Loaded Structures on Sandy Seabed

More complicated situations may occur in the sand around a pipeline (Palmer et al. 2004; Damgaard et al. 2006), a caisson breakwater, or another structure on top of or partly in the seabed. Seabed and structure are simultaneously loaded by the waves. The loading of the sand around the structure is thus loaded in two different ways: directly and indirectly via the structure. The indirect loading of a sand element differs in several ways from the direct one:

1. It is asymmetric rather than symmetric.
2. The spatial variation in amplitude, mean value, and directions is often stronger, especially with structures like pipelines with dimensions much smaller than the wavelength and near the edges of structures like caissons.
3. The shear stress amplitudes are usually significantly stronger close to the structure. This may be compensated for by much larger initial vertical effective stresses underneath the middle of a large structure. Near the edges, however, the relative shear stresses can be much higher.
4. Instantaneous pore pressures may be relatively important in the case of nearly incompressible pore water.

The asymmetry allows for behavior as sketched in Fig. 24 with partial liquefaction and cyclic mobility. This may lead to failure due to stepwise, residual deformation, rather than liquefaction flow failure in the case of caisson breakwaters founded on sand (Kudella and Oumeraci 2004; De Groot et al. 2006; Kudella et al. 2006).

The spatial variation causes a strong interaction between adjacent sand elements. Some elements may be "fluidized" by the excess pore pressures generated in neighboring elements. Stresses are redistributed from elements weakened by liquefaction to elements that show less liquefaction and thus do not lose so much of their stiffness. Many practically liquefied sand elements underneath a structure do not necessarily endanger its foundation stability as a whole if enough nonliquefied elements remain.

The higher stresses and stress amplitudes cause the indirect loading to dominate the direct loading close to the structure completely in most cases. This is clearly demonstrated for caisson breakwaters by Kudella and Oumeraci (2004) or Kudella et al. (2006), who use the terms "caisson motion mode" and "wave motion mode" for indirect, respectively, direct loading. This allows for a laboratory setup in which the wave is not modeled and no wave flume is needed provided the load to the structure is well simulated (Foray et al. 2006). Examples of such situations are also described in Dunn et al. (2006), Chap. 3 of Oumeraci et al. (2001), and Kvalstad and De Groot (1999).

A special case, more extensively discussed in Teh et al. (2006) and Foray et al. (2006), is illustrated in Fig. 37: a pipeline so heavily loaded that it moves strongly. Three zones of excess pore pressure may be distinguished. Close to the pipeline strong deformations and plasticity may be observed including strong instantaneous excess pore pressure fluctuations (Zone I). Small, elastic deformations with limited instantaneous pore pressure fluctuations may characterize the zone at a large distance (Zone III). In the intermediate Zone II, moderate, mainly elastic deformations may be combined with some residual pore pressures and densification, due to the relatively long drainage distance, and especially if the extreme waves have a limited duration.

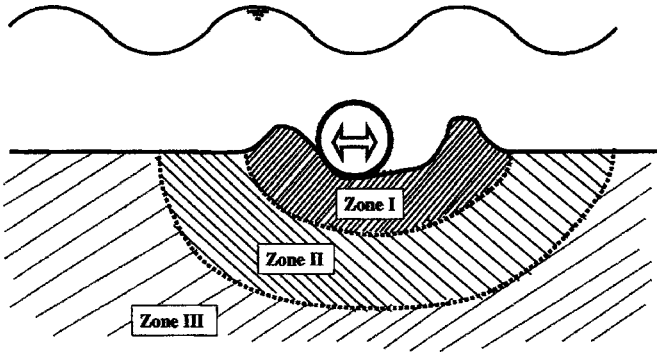

Fig. 37. Three excess pore pressure zones around strongly moving pipeline

Densification of Sandy Seabed

Several techniques are available to densify sandy seabeds: vibroflotation, blasting, plate vibration, and dynamic consolidation (Ménard). They are all based on the same principle as the development of wave induced excess pore pressures: induce the tendency of the soil skeleton to contract by means of cyclic shearing, often in combination with compressive normal stress, and let the excess pore water drain off to the surface. None of the methods is successful in soil with many fines, because the fines prevent this drainage and prevent the desired decrease in pore volume.

Summary of Liquefaction Phenomena and Their Physics

Types of Liquefaction

The term liquefaction can be used for complete liquefaction, i.e., the complete loss of effective stress, and also for partial liquefaction, i.e., the generation of excess pore pressures.

Two main types of (partial) liquefaction can be distinguished, one of which can be subdivided in two subtypes:

1. Liquefaction due to monotonic loading; and
2. Liquefaction due to cyclic loading, with the two subtypes:
   - Instantaneous (or momentary or transient) liquefaction; and
   - Residual liquefaction.

Apart from these main types, the following excess pore pressures phenomena should be mentioned:

1. Cyclic mobility, which can be considered as a partial liquefaction due to cyclic loading combining elements of instantaneous and residual liquefaction; and
2. Negative excess pore pressures during fast changing monotonic loading.

Physical Cause of Liquefaction and Its Consequences

The physics of liquefaction phenomena in sandy soils around marine structures is strongly related to loading induced tendency of volume strain of the soil skeleton and the resistance to such volume strain by pore water. This resistance, and the consequent risk of liquefaction, is strongest in undrained conditions with incompressible pore water. Consequently, liquefaction phenomena are influenced by the following factors:

- Loading characteristics (level; shear or normal; stationary, fast or cyclic);
- Sensitivity to volume strain of the soil skeleton;
- Compressibility of pore water; and
- Soil permeability and drainage distance.

Instantaneous Liquefaction

Most important for instantaneous liquefaction are:

1. Amplitude and period of the load;
2. Ratio between the elastic compressibility of the soil skeleton and the compressibility of the pore water;
3. The absolute value of the highest of both compressibilities; and
4. Soil permeability and drainage distance.

Load period, compressibility, permeability, and drainage distance can often be combined in one nondimensional parameter, such as d/z_2, where d is the length of a characteristic flow path and $z_2=\sqrt{(c_{ve}T/\pi)}$.

Complete instantaneous liquefaction is highly unlikely with incompressible pore water. On the contrary, strong amplitude damping with depth, phase shift with depth, and large pressure gradients near the seabed are typical for relatively compressible pore water. Coastal soils exposed to tides often have a significant amount of air/gas, the presence of which significantly increases the risk of wave induced instantaneous liquefaction.

Residual Liquefaction

Residual excess pore pressures are not really residual, but are called this because they have a much longer duration than instantaneous excess pore pressures. Most important for residual liquefaction are:

1. CSSR, largely determined by load amplitude and initial vertical effective stress;
2. Sensitivity to contraction of the soil skeleton, largely depending on the relative density, and the elastic compressibility of the soil skeleton, slightly depending on the relative density;
3. Duration of the loading (earthquake, storm, extreme part of storm) and the loading frequency, especially in relation with:
4. Soil permeability and drainage distance.

Loading duration, compressibility, permeability, and drainage distance can often be combined in a similar nondimensional parameter as with instantaneous liquefaction, if the load period is replaced with the loading duration. The sensitivity to contraction is also influenced by the way sedimentation has taken place, aging, preshearing, and in a laboratory, sample handling.

The influence of the grain size distribution on the stress–strain relationship of the skeleton of noncohesive soils is limited to the influence of the gradation. Well-graded sand shows larger contraction, but also larger compressibility, factors which largely compensate each other in the generation of excess pore pressures.

A more important influence of the grain size distribution on liquefaction goes through the sizes of the smaller grains and the strongly correlated permeability. It is often stated that liquefaction cannot occur in soils finer than silt and larger than sand. The lower limit is probably due to cohesion which becomes important with a significant portion of very fine, plastic particles. See, however, De Wit (1995). The consequences of excess pore pressures in cohesive soil are not as significant as with cohesionless soil. The upper limit is probably only due to drainage. Gravels can be contractive, but liquefaction can only occur if the gravel layers are very thick or if they are surrounded by poorly draining boundaries.

Difference in load duration and load frequency cause a large difference between earthquake induced and wave induced residual liquefaction. That no complete liquefaction occurs with many earthquakes is due to the limited number of load cycles. That no complete liquefaction occurs with many storms, is often due to drainage and increase in resistance to pore pressure generation caused by densification.

The gas content of the pore fluid reduces the risk of residual liquefaction.

Combinations of Instantaneous and Residual Liquefaction

High and relatively short waves may cause very high shear stress amplitudes in a sandy seabed and a very special combination of instantaneous pore pressure fluctuation and residual liquefaction. The pore pressure fluctuation is induced by alternating dilation and contraction. With constant wave loading, the inflow discharge of water during dilation equals the outflow discharge during contraction, yielding constant residual excess pore pressures. The residual excess pore pressures nearly correspond to complete liquefaction.

Another special combination of instantaneous and residual excess pore pressures may occur in relatively dense sand underneath wave loaded structures at locations where the shear loading is strongly asymmetric. Here, instantaneous pore pressures may also be caused (partly) by alternating dilation and contraction. No drainage is needed to reach a constant partial residual liquefaction or even a negative residual liquefaction. Such a situation may, however, go along with continuing shear deformation: cyclic mobility.

Acknowledgments

This study was partially funded by the European Commission Research Directorate, FP5, specific program "Energy, Environment and Sustainable Development," Contract No. EVK3-CT-2000-00038, Liquefaction Around Marine Structures LIMAS. ⟨http://vb.mek.dtu.dk/research/limas/limas.html⟩. Another part was funded by Delft Cluster, performing fundamental research for sustainable delta development. Delft Cluster is established by six institutes in Delft, The Netherlands.

Notation

The following symbols are used in this paper:

a = acceleration (m/s^2);
CSSR = $\Delta\tau/\sigma'_{v0}$=cyclic shear stress ratio [−];
c_{ve} = $k/\{\gamma_w(\alpha+n\beta)\}$, elastic component of consolidation coefficient (m^2/s);
d = thickness of soil layer (m);
E_{OED} = $1/m_v$=stiffness in primary loading of oedometer test (N/m^2);
e = $n/(1-n)$=void ratio [−];
$e_{crit\ state}$ = void ratio in critical state [−];
e_{max} = maximum void ratio (according to some standard procedure);

e_{min} = minimum void ratio (according to some standard procedure);
G = shear modulus (N/m^2);
G_{50} = shear modulus as defined in Fig. 4 (N/m^2);
g = acceleration of gravity (m/s^2);
I_D = $(e_{max}-e)/(e_{max}-e_{min})$=density index (≈relative density) [−];
i = head gradient [−];
K = elastic compression modulus (or 'bulk modulus') of skeleton (N/m^2);
K_{ref} = reference value of K for $\sigma'_{oct}=\sigma'_{ref}$($N/m^2$);
K_{VIRGIN} = compression modulus of skeleton in virgin loading: plastic+elastic (N/m^2);
K_w = $1/\beta$=elastic compression stiffness of pore water (N/m^2);
k = permeability of sand (m/s);
L = wave length (m);
M = E_{OED}=stiffness in primary loading of oedometer test (N/m^2);
N = number of cycles [−];
N_L = number of cycles to liquefaction in undrained cyclic test [−];
n = $e/(1+e)$=porosity [−];
n_{max} = maximum porosity (according to some standard procedure);
n_{min} = minimum porosity (according to some standard procedure);
T = wave period (s);
$T_{CHAR,DRAIN}$ = characteristic drainage period (s) for wave-induced liquefaction;
t = time (s);
u = excess pore-water pressure, i.e., difference between actual pore pressure and hydrostatic pressure for still water level (N/m^2);
v = cutting speed;
y = power indicating influence of mean effective stress on K;
z = depth below seabed (m);
z_1 = $L/2\pi$=characteristic length for pore pressure amplitude damping in case of incompressible pore water (m);
z_2 = $\sqrt{(c_{ve}T/\pi)}$=characteristic length for pore pressure amplitude damping due to elastic storage (m);
α = $1/(K+4G/3)$=elastic compressibility for one-dimensional restrained deformation (m^2/N);
β = $1/K_w$=elastic compressibility of pore water (m^2/N);
γ = shear strain in plane where it is largest [−];
γ' = $(\rho-\rho_w)g$=submerged unit weight of soil (N/m^3);
γ_w = $\rho_w g$=unit weight of water (N/m^3);
ε_v = vertical strain [−];
ε_{vol} = volume strain [−];
ρ = density of soil (grains and pore fluid) (kg/m^3);
ρ_w = density of water (kg/m^3);
σ = (total) normal stress (N/m^2);
σ' = effective normal stress (N/m^2);
σ'_{oct} = $(\sigma'_1+\sigma'_2+\sigma'_3)/3$=mean effective stress ($N/m^2$);
σ'_{ref} = reference value of stress for influence of σ'_{oct} on K(N/m^2);
σ_v = vertical total stress (N/m^2);
σ'_v = vertical effective stress (N/m^2);
σ'_{v0} = original vertical effective stress (before excess pore pressure starts) (N/m^2);
$\sigma_1,\sigma_2,\sigma_3$ = principal stresses (N/m^2);
τ = shear stress (N/m^2);
φ = friction angle [−]; and
ψ = dilation angle [−].

References

Castro, G. (1975). "Liquefaction and cyclic mobility of saturated sands." *J. Geotech. Eng. Div., Am. Soc. Civ. Eng.*, 101(6), 551–569.

Damgaard, J. S., Foray, P., Palmer, A. C., Sumer, B. M., and Fredsøe, J. (2006). "Guidelines for pipeline on-bottom stability on liquefied seabeds." *J. Waterw., Port, Coastal, Ocean Eng.*, 132(4), 300–309.

De Groot, M. B., Lindenberg, J., and Meijers, P. (1991). "Liquefaction of sand used for soil improvement in breakwater foundation." *Proc., Geo-Coast'91 Conf.*, Yokohama, Japan, 555–560.

De Groot, M. B., Kudella, M., Meijers, P., and Oumeraci, H. (2006). "Liquefaction underneath marine gravity structures subjected to wave loads." *J. Waterw., Port, Coastal, Ocean Eng.*, 132(4), 325–335.

De Groot, M. B., and Meijers, P. (1992). "Liquefaction of trenchfill around a pipeline in the seabed." *Proc. BOSS-92 Conf.*

De Wit, P. J. (1995). "Liquefaction of cohesive sediments caused by waves." Ph.D. thesis, *Rep. No. 95-2, Communications on Hydraulic and Geotechnical Engineering*, Delft University Press, Delft, The Netherlands.

Dunn, S., Vun, P. L., Chan, A., and Damgaard, J. S. (2006). "Numerical modeling of liquefaction around pipelines." *J. Waterw., Port, Coastal, Ocean Eng.*, 132(4), 276–288.

Foray, P., Bonjean, D., Michallet, H., and Mory, M. (2006). "Fluid–soil–structure interaction in liquefaction around a cyclically moving cylinder." *J. Waterw., Port, Coastal, Ocean Eng.*, 132(4), 289–299.

Ibsen, L. B. (1994). "The stable state in cyclic triaxial testing on sand." *Soil Dyn. Earthquake Eng.*, 13, 63–72.

Ishihara, K. (1993). "Liquefaction and flow failure during earthquakes." *Geotechnique*, 43(3), 351–415.

Ishihara, K., Tatsuoka, F., and Yasuda, S. (1975). "Undrained deformation and liquefaction of sand under cyclic stresses." *Soils Found.*, 15(1), 29–44.

Kudella, M., and Oumeraci, H. (2004). "Wave-induced transient and residual pore pressure in the sand bed underneath a caisson breakwater—Processes leading to liquefaction." *Cyclic behaviour of soils and liquefaction phenomena*, Triantafyllidis, ed., Balkema, Leiden, The Netherlands, 411–424.

Kudella, M., Oumeraci, H., De Groot, M. B., and Meijers, P. (2006). "Large-scale experiments on pore pressure generation underneath a caisson breakwater." *J. Waterw., Port, Coastal, Ocean Eng.*, 132(4), 310–324.

Kvalstad, T. J., and De Groot, M. B. (1999). "Degradation and residual pore pressures." *Probabilistic design tools for vertical breakwaters—Geotechnical aspects. MAST III-PROVERBS-project*, M. B. De Groot, ed., Technische Universität Braunschweig Press, Braunschweig, Germany.

Luong, P. (1980a). "Phénomènes cycliques dans les sols pulvérulents." *Rev. Fr. Géotech.*, 10, 39–53.

Luong, P. (1980b). "Stress-strain aspects of cohesionless soils under cyclic and transient loading." *Proc., Int. Symp. on Soils under Cyclic and Transient Loading*, Vol. 1, Swansea, Balkema, Rotterdam, The Netherlands, 315–324.

Marcuson, W. F., III. (1978). "Definition of terms related to liquefaction." *J. Geotech. Eng. Div., Am. Soc. Civ. Eng.*, 104(9), 1197–1200.

Mory, M., et al. (2006). "Field study of momentary liquefaction caused by waves around a coastal structure." *J. Waterw., Port, Coastal, Ocean Eng.*, in press.

Ottesen Hansen, N. E. (2006). "Bearing capacity of sand during partially drained conditions caused by impulsive loads." *J. Waterw., Port, Coastal, Ocean Eng.*, in press.

Oumeraci, H., Kortenhaus, A., Allsop, N. W. H., De Groot, M. B., Crouch, R. S., Vrijling, J. K., and Voortman, H. G. (2001). *Probabilistic design tools for vertical breakwaters*, Balkema, Lisse, The Netherlands.

Palmer, A. C. (1999). "Speeds effects in cutting and ploughing." *Geotechnique*, 49(3), 285–294.

Palmer, A. C., Teh, T. C., Bolton, M. D., and Damgaard, J. S. (2004). "Stable pipelines on unstable seabed: Progress towards a rational design method." *Proc., Offshore Pipeline Technology Conf.*, Amsterdam, The Netherlands.

Richwien, W., and Perau, E. (1999). "Pore pressure and soil pressure in sandy subsoil beneath a caisson." *MAST III—PROVERBS-project*, University of Essen, Institut für Grundbau und Bodenmechanik, Germany.

Sawicki, A., and Mierczynski, J. (2006). "Developments in modeling liquefaction of granular soils, caused by cyclic loads." *Appl. Mech. Rev.*, 59(2), 91–106.

Sawicki, A., and Swidzinski, W. (1989). "Pore pressure generation, dissipation and resolidification in saturated subsoil." *Soils Found.*, 29(4), 62–74.

Sawicki, A., and Swidzinski, W. (2006). "Modelling of liquefaction-related phenomena in the 1999 Kocaeli Earthquake." *J. Waterw., Port, Coastal, Ocean Eng.*, in press.

Smits, F. P., Andersen, K. H., and Gudehus, G. (1978). "Pore pressure generation." *Proc., Int. Symp. on Soil Mech. Research and Found. Design for the Oosterschelde Storm Surge Barrier*, Vol. 1 Delft, The Netherlands, II.3.

Stoutjesdijk, T. P., De Groot, M. B., and Lindenberg, J. (1998). "Flow slide prediction method: influence of slope geometry." *Can. Geotech. J.*, 35, 34–54.

Sumer, B. M., and Fredsøe, J. (2002). *The mechanics of scour in the marine environment*, World Scientific, River Edge, N.J.

Sumer, B. M., Fredsøe, J., Christensen, S., and Lind, M. T. (1999). "Sinking/floatation of pipelines and other objects in liquefied soil under waves." *Coastal Eng.*, 38, 53–90.

Sumer, B. M., Truelsen, C., and Fredsøe, J. (2006). "Liquefaction around pipelines under waves." *J. Waterw., Port, Coastal, Ocean Eng.*, 132(4), 266–275.

Teh, T. C., Palmer, A. C., and Bolton, M. D. (2004). "Wave-induced seabed liquefaction and the stability of marine pipelines." *Cyclic behaviour of soils and liquefaction phenomena*, Triantafyllidis, ed., Balkema, Leiden, The Netherlands, 449–453.

Teh, T. C., Palmer, A. C., Bolton, M. D., and Damgaard, J. (2006). "Stability of submarine pipelines on liquefied seabeds." *J. Waterw., Port, Coastal, Ocean Eng.*, 132(4), 244–251.

Teh, T. C., Palmer, A. C., and Damgaard, J., Bolton, M. D. (2003). "Experimental study of marine pipelines on unstable and liquefied seabed." *Coastal Eng.*, 50, 1–17.

Vaid, Y. P., and Chern, J. C. (1983). "Effect of static shear on resistance to liquefaction." *Soils Found.*, 23(1), 47–60.

van Os, A. G., and van Leussen, W. (1987). "Basic research on cutting forces in saturated sand." *J. Geotech. Eng.*, 113(12), 1501–1516.

Verruijt, A. (1982). "Approximations of cyclic pore pressures caused by sea waves in a poro-elastic half-plane." *Soil mechanics—Transient and cyclic loads*, G. N. Pande and O. S. Zienkiewicz, eds., Chap. 3, Wiley, Chichester, U.K., 37–51.

Yamamoto, T., Koning, H. L., Sellmeijer, H., and Van Hijum, E. (1978). "On the response of a poro-elastic bed to water waves." *J. Fluid Mech.*, 87(1), 193–206.

Youd, T. L., et al. (2001). "Liquefaction resistance of soils: Summary report from the 1996 NCEER and 1998 NCEER/NSF workshops on evaluation of liquefaction resistance of Soils." *J. Geotech. Geoenviron. Eng.*, 127(10), 817–833.

Zen, K., and Yamazaki, H. (1990a). "Mechanism of wave-induced liquefaction and densification in seabed." *Soils Found.*, 30(4), 90–104.

Zen, K., and Yamazaki, H. (1990b). "Oscillatory pore pressure and liquefaction in seabed induced by ocean waves." *Soils Found.*, 30(4), 147–161.

Zen, K., and Yamazaki, H. (1991). "Field observation and analysis of wave-induced liquefaction in seabed." *Soils Found.*, 31(4), 161–179.